What affects the predictability of evolutionary constraints using a G-matrix? The relative effects of modular pleiotropy and mutational correlation

Chebib, Jobran ; Guillaume, Frédéric

Abstract: Phenotypic traits do not always respond to selection independently from each other and often show correlated responses to selection. The structure of a genotype-phenotype map (GP map) determines trait covariation, which involves variation in the degree and strength of the pleiotropic effects of the underlying genes. It is still unclear, and debated, how much of that structure can be deduced from variational properties of quantitative traits that are inferred from their genetic (co)variance matrix (G-matrix). Here we aim to clarify how the extent of pleiotropy and the correlation among the pleiotropic effects of mutations differentially affect the structure of a G-matrix and our ability to detect genetic constraints from its eigen decomposition. We show that the eigenvectors of a G-matrix can be predictive of evolutionary constraints when they map to underlying pleiotropic modules with correlated mutational effects. Without mutational correlation, evolutionary constraints caused by the fitness costs associated with increased pleiotropy are harder to infer from evolutionary metrics based on a G-matrix's geometric properties because uncorrelated pleiotropic effects do not affect traits' genetic correlations. Correlational selection induces much weaker modular partitioning of traits' genetic correlations in absence then in presence of underlying modular pleiotropy.

DOI: https://doi.org/10.1111/evo.13320

What affects the predictability of evolutionary constraints using a **G**-matrix? The relative effects of modular pleiotropy and mutational correlation.

Jobran Chebib and Frédéric Guillaume

Department of Evolutionary Biology and Environmental Studies, University of Zürich, Winterthurerstrasse 190, CH-8057 Zürich, Switzerland. email: jobran.chebib@ieu.uzh.ch

Abstract

Phenotypic traits do not always respond to selection independently from each other and often show correlated responses to selection. The structure of a genotype-phenotype map (GP map) determines trait covariation, which involves variation in the degree and strength of the pleiotropic effects of the underlying genes. It is still unclear, and debated, how much of that structure can be deduced from variational properties of quantitative traits that are inferred from their genetic (co)variance matrix (**G**-matrix). Here we aim to clarify how the extent of pleiotropy and the correlation among the pleiotropic effects of mutations differentially affect the structure of a **G**-matrix and our ability to detect genetic constraints from its eigen decomposition. We show that the eigenvectors of a **G**-matrix can be predictive of evolutionary constraints when they map to underlying pleiotropic modules with correlated mutational effects. Without mutational correlation, evolutionary constraints caused by the fitness costs associated with increased pleiotropy are harder to infer from evolutionary metrics based on a **G**-matrix's geometric properties because uncorrelated pleiotropic effects do not affect traits' genetic correlations. Correlational selection induces much weaker modular partitioning of traits' genetic correlations in absence then in presence of underlying modular pleiotropy.

Keywords: Pleiotropy, Modularity, Genotype-Phenotype map, Mutational Correlation, Evolvability, G-matrix

This article has been accepted for publication and undergone full peer review but has not been through the copyediting, typesetting, pagination and proofreading process, which may lead to differences between this version and the Version of Record. Please cite this article as doi: 10.1111/evo.13320

Introduction

Although predicting the evolutionary responses of traits to selection is of great interest in evolutionary biology, it is not straight-forward because traits do not always evolve autonomously [50, 15, 54, 62, 72, 74, 1]. Practically, this is significant in selective breeding where selection on particular traits may be hampered by underlying genetic dependencies and cause correlated responses for undesired effects [89, 23, 47]. The evolutionary trajectories of any traits may not be independent of one another if pleiotropy or linkage disequilibrium in their underlying genes create covariation between the phenotypic traits [49, 3, 25, 85]. Pleiotropy may constrain the evolution of separate traits by two mechanisms. First, the net fitness effect of a mutation beneficial for the adaptation of a particular trait will be decreased proportionally to the number of traits it pleiotropically affects (its pleiotropic degree) because its deleterious side-effects will be larger, slowing the rate of adaptation compared to genetically independent traits [64, 88] [but see 82, for evidence of a positive correlation between mutational effect size and pleiotropic degree, which may mitigate the "cost of pleiotropy"]. Second, by generating genetic correlation among traits, pleiotropic mutations may divert the population's response to selection away from its path of maximum fitness increase [48, 3, 74]. These can be seen as two separate effects because pleiotropy may not always result in genetic or phenotypic correlations if uncorrelated pleiotropic effects at different loci cancel each other out, a case called hidden pleiotropy [80, 5]. Even without causing correlated trait responses, the deleterious side effects of pleiotropic mutations may still constrain evolutionary responses by decreasing the additive genetic variance of each trait (when under stabilizing selection) compared to its single trait expectation [78]. Genetic dependencies underlying traits may thus sometimes be detected from trait covariation, although not always. Correctly interpreting evolutionary inferences that can be drawn from patterns of trait covariation depend on the details of the genotype-to-phenotype (GP) map, that is, on how genetic variation and trait variation are connected. Therefore, understanding how the structure of a GP map affects the potential evolutionary responses to

selection of a focal trait is essential [35].

Information on trait evolutionary dependencies within a population can be gleaned from trait genetic co-variation encapsulated in the matrix of additive genetic variance-covariance, the **G**-matrix. The **G**-matrix is a central tool in quantitative genetics because it is used to predict the multivariate response to selection of a set of traits with the multivariate breeder's equation, $\boldsymbol{\Delta}\bar{\boldsymbol{z}} = \mathbf{G}\boldsymbol{\beta}$, where $\boldsymbol{\Delta}\bar{\boldsymbol{z}}$ is the vector of the changes in mean population trait values and $\boldsymbol{\beta}$ is the vector of selection gradients acting on each trait [48]. The misalignment of the response vector with the selection gradient vector is evidence of an evolutionary constraint–the population does not evolve along the path of maximum increase in fitness, represented by $\boldsymbol{\beta}$. Furthermore, genetic correlations among phenotypic traits may cause the reduction of genetic variance for specific combination of traits, with, in the most extreme case, complete absence of adaptive variation and thus no response to selection in a specific direction of phenotypic space on which selection may act [i.e., an absolute constraint corresponding to an eigenvector with a null eigenvalue, 12]. The distribution of genetic variation in multivariate trait space is obtained from the diagonalization (eigen decomposition) of the **G**-matrix, with $\boldsymbol{g}_{max}$ the first eigenvector (first principal component) and the direction of greatest genetic co-variation of the traits, and thus of greatest response to selection [also called the "line of least resistance" by 74]. Therefore, the eigen decomposition of **G** is commonly used to infer evolutionary constraints in multivariate trait space. For example, an analysis of adaptive morphological changes in freshwater stickleback populations by Schluter [74] suggested that the adaptive trajectories of diverging populations were biased towards $\boldsymbol{g}_{max}$, more strongly so at the beginning of their history of divergence than later [but see 7, for an alternative explanation]. Similar evolutionary constraints imputed to $\boldsymbol{g}_{max}$ have been reported in empirical studies [11, 6, 52, 75], while others argued against such a role [57, 55, 9, 84]. Present-day orientation of $\boldsymbol{g}_{max}$ in phenotype space may, however, not correctly inform about past constraints since genetic covariance may have evolved. Focusing mostly on $\boldsymbol{g}_{max}$ orientation may also be misleading because other trait axes (eigenvectors) may bear sufficient genetic variation to yield high evolvability and sustain adaptation in directions unbiased by $\boldsymbol{g}_{max}$, yet still biasing selection responses [38].

The inference of genetic constraints from the eigen structure of the G-matrix has been criticized on two main grounds. First, trait genetic covariation is influenced by all evolutionary processes that affect allele frequencies

and the covariation of allelic values in a population (e.g., linkage [49], drift [27], mutation and selection [41, 87, 56], migration [31], phenotypic plasticity [21]). Changes in allele frequencies may change genetic covariance among traits and the shape of a **G**-matrix through time, and thus modify the orientation and the length of the eigenvectors of **G**, making predictions of evolutionary trajectories based on the multivariate breeders equation valid only on the short term [79]. However, how sensitive the shape of a **G**-matrix is to changes caused by those evolutionary forces depends on the strength of the pleiotropic links among traits, and thus on the details of the GP map [49]. For instance, previous theoretical studies showed that strong correlation of mutational pleiotropic effects (i.e., how similar are shared mutational effects on traits) stabilizes trait covariance across generations [41, 31, 4], which may stabilize the **G**-matrix on evolutionary times and across taxa [77].

The second criticism is linked to the implicit assumption that trait covariation is caused by the pleiotropic nature of the genetic underpinnings of the traits. However, how much the principal components of **G** reveal of the underlying molecular structure of the GP map is unclear, if not controversial. Often, trait phenotypic correlations are interpreted as evidence of the genetic integration of those traits in functional or developmental genetic modules. For instance, pleiotropic effects of quantitative trait loci (QTL) affecting mouse cranial and mandibular morphological traits cluster together relative to basal developmental modules [58], but not to phenotypic modules determined from trait genetic correlations [73]. This lack of correspondence and the inherent difficulty of inferring genetic details from patterns of population variation can be a consequence of the constant rewriting of trait relationships by a multitude of overlapping developmental and functional processes [33, 65]. Nevertheless, if patterns of trait covariation are grounded in modular pleiotropic effects, they may remain constant across populations and species [77, 59] and durably affect evolutionary trajectories [74]. Under such circumstances, eigenvectors of a **G**-matrix may reveal the underlying modules of pleiotropic effects [59]. But that idea, and the utility of **G**-matrix diagonalization, have been challenged [28, 13, 8]. In particular, Berner [8] used simulations to argue that trait loading on eigenvectors of a **G**-matrix cannot be used to gain knowledge of the underlying genetic architecture of pleiotropic loci and showed that the eigenvectors were often not stable across replicates, casting doubt on their predictive utility. Unfortunately, that study did not model variation in mutational correlation of pleiotropic loci, assuming it to be perfect, and focused on the interpretation

of the sign of the trait loading on the eigenvectors of the **G**-matrix, which are arguably not representative of the sign of the pleiotropic effects of the underlying loci. While we generally agree that a link between a **G**-matrix and its GP map should not be taken for granted, we argue here that meaningful inferences about the genetic underpinnings of phenotypic covariation can be made between populations or species with similar functional relationships among traits [81, 77, 59].

The **G**-matrix is undoubtedly an important tool to predict short-term population responses to selection and the study of its geometrical properties (its shape) can teach us about the relationship between traits and their evolutionary potentials. Absence of trait covariation within a **G**-matrix causes it to resemble a hyper-sphere with axes (the eigenvectors) roughly equal in magnitude (when trait variance is equal) and aligned with the trait axes, which indicates the absence of directional constraint on the evolution of the original traits. Genetic correlations among those traits cause the hyper-sphere to elongate and tilt along the axes bearing the most genetic variation and corresponding to orthogonal combinations of correlated traits, resulting in an hyper-ellipsoid. The eigenvectors are then orthogonal phenotypes on which selection may act independently, with few bearing the majority of the variation present in the original traits and others with much reduced variation leading to a reduction of phenotypic dimensionality [e.g. 47]. Understanding of how the dimensionality of the phenotypes stems from the dimensionality of mutational variation is important to understand the evolvability of organisms. From Fisher-Orr population genetic model of adaptation [26, 64], a lower dimensionality (reduced number of traits under selection) reduces the so-called "cost of complexity" caused by pleiotropic mutations. Martin and Lenormand [53] showed that more correlated mutational effects among traits reduces that cost when the resulting mutational variance-covariance matrix (**M**-matrix) has few eigenvectors bearing most of the variation among traits, **and** selection and mutations act on all traits. Yet, the distribution of fitness effects of pleiotropic mutations depend more on the total number of traits they affect than the total number of traits of an organism, when pleiotropic effects are restricted among subsets of the traits [17, 51]. So far, most studies of the evolution of the **G**-matrix have modeled simplistic GP maps where all genes affect all traits (i.e., universal pleiotropy) with variation in trait correlation driven, in part, by variation in the correlation among pleiotropic mutational effects. In contrast, little effort has been devoted to understanding how variation in the pleiotropic degree of loci and the modular organization

of pleiotropic effects within the GP map affect the structure and stability of the **G**-matrix and the evolvability of traits under directional selection, even though variable pleiotropy seems widespread and often modular in nature [86, 83].

Here, we are interested in how such variation in the organization of pleiotropic links within the GP map and the correlation of allelic pleiotropic effects affect the genetic covariation of the traits. We use computer simulations to investigate the conditions under which modular pleiotropy in the GP map translates into detectable modularity in the **G**-matrix. We further investigate whether evolutionary metrics capture modular variation in the GP map from the observed eigen structure of the resulting **G**-matrices. Lastly, we examine the effect of GP map modularity on the evolutionary rate and trajectory of traits under directional selection. We show that inferences from evolutionary metrics can capture variation in the modularity of the GP map from the eigen structure of the **G**-matrix provided some level of pleiotropic mutational correlation is present.

Methods

Simulation development

We implemented the capability for non-universal pleiotropy into the individual-based, forward-in-time population genetics simulation software **Nemo** (v2.3.4) [30]. To this end, we first allowed loci underlying quantitative traits to map to a subset of the traits modeled by providing a *loci* $\times$ *traits* input binary matrix (connectivity matrix). This modification permits the implementation of modular structures in the GP map of modeled traits. Second, each locus may have its own mutational effect distribution commensurate with the number of traits it affects (pleiotropic degree). This permits mutational variances (and covariances) for each locus to be based on its pleiotropic degree, which can ensure that total genomic mutational variances are comparable between traits pertaining to different modules. Both of these modifications were necessary for comparing GP maps with different module sizes and their resulting **G**-matrices.

Experimental design

To determine how GP map modularity with or without mutational correlation affects the structure of the **G**-matrix and the ability of its traits to respond to selection, we modeled five different sets of modular GP mappings by varying the degree of pleiotropy between 120 additive loci and 12 quantitative traits (Figure 1). The twelve traits were divided among the loci to create five degrees of modularity with an equal number of loci per module and trait. The modularity varied from 1 module of 12 traits to 6 modules of 2 traits with intermediate values of 2, 3, and 4 modules. The number of loci per trait then varied from 120 (modularity 1) to 20 (modularity 6), with intermediate values of 60, 40, and 30 for modularity 2, 3, and 4, respectively. Consequently, the pleiotropic degree of each locus in the GP map corresponded to the number of traits in each module, and each trait was affected by less loci when the modularity was larger.

Mutational effects at each locus were drawn from a multivariate normal distribution with number of dimensions equal to the pleiotropic degree of the loci within a module, and varying covariation (see mutational correlation below). The per-locus mutation variance-covariance matrix, the **M**-matrix, described the amount of mutational effect variation on each trait and the effect covariance between traits. An **M**-matrix was set for each locus within each trait module and was used to parameterize the distribution from which new allelic effects were drawn.

Mutational effects were then added to the existing allelic values [continuum-of-allele model; 20]. We set the correlation of mutational effects equal between the traits within each module but mutations had no effects across modules. Mutational correlation values used were $r_\mu = 0$, 0.25, 0.5, and 0.75 ($r_\mu = 0$ meant that mutations still affected more than one trait but those mutational effects were uncorrelated). Average mutational contribution to total genetic variance of a trait in a module was equalized across different modularity sets by adjusting the mutational variance (and covariance) of loci dependent on their pleiotropic degrees. The total mutational variance of a trait is $V_m = 2L\mu\alpha^2$, with L diploid, additive loci having average effect size α^2 and mutating at rate 2μ. We set $\mu = 0.0001$ and varied α^2 keeping $V_m = 0.00024$ independent of L (e.g., $\alpha^2 = 0.04$ across all loci for modularity 4 and 0.02 across all loci for modularity 2). All loci (and traits and modules) were then expected to have the same mutational (and genetic) variance for a given modularity, allowing for direct comparisons across the different

modularity sets of the GP map. We assumed no linkage among loci (free recombination), and no environmental effects on the traits.

Unless otherwise specified, each simulation was run with 5,000 initially monomorphic (variation is introduced through mutations) individuals for 10,000 generations achieving mutation-selection balance in order to observe general patterns of genetic variation from the resulting **G**-matrices. Individuals were hermaphrodites mating at random within a population, with non-overlapping generations. Phenotypes were calculated for each trait by summing the allelic values of all loci affecting that trait. Gaussian stabilizing selection was applied and determined the survival probability of juveniles, whose fitness was calculated as $w = \exp\left[-\frac{1}{2}\left((\mathbf{z}-\Theta)^{\mathrm{T}} \cdot \Omega^{-1} \cdot (\mathbf{z}-\Theta)\right)\right]$, where $\mathbf{z}$ is the individual phenotype vector, Θ is the vector of local optimal trait values (set to 5 for all traits), and Ω is the selection variance-covariance matrix ($n \times n$, for n traits) describing the multivariate Gaussian selection surface. The Ω matrix was set as a diagonal matrix with diagonal elements $\omega^2 = 10$, and off-diagonal set to zero when selection was not correlated (see below for correlational selection). The strength of selection scales inversely with ω^2. An ω^2 value of 10 corresponds to an empirical estimate of the strength of quadratic selection acting on quantitative traits from Kingsolver et al. [46].

In order to compare the effects of mutational correlation with the effects of correlational selection on the **G**-matrix's eigen structure, we modeled correlational selection in two separate sets of simulations. In the first scenario, we added modular correlational selection between traits while keeping the same GP maps as described above (same pleiotropic degree of the loci) but without mutational correlation. Correlational selection is modeled by giving non-zero values to the off-diagonal terms in the selection matrix, Ω, following the modular structure of the GP map. In the second scenario, we applied the same modular correlational selection on the traits while removing the modularity in the GP map (i.e. imposing universal pleiotropy on all loci) also without mutational correlation. We used three strengths of correlational selection ($r_\omega = 0.25$, 0.5, or 0.75). Overall, we ran fifty replicates of each simulation for all combinations of three stabilizing selection regimes, five modularities, and mutational and selection correlation values. Statistics were averaged over all replicates at the last generation of each run.

Measuring G-matrix decomposition structure

Several metrics were implemented to measure how the structure of the **G**-matrix is affected by combinations of different pleiotropic modularities, mutational correlations, and selection correlations. We calculated the eigenvalues and eigenvectors from the diagonalization of the **G**-matrix of each simulation after 10,000 generations of stabilizing selection. Stability of the orientation of eigenvectors among replicates was evaluated by measuring the co-linearity (the cosine of the angle) between eigenvectors and each module's unit vector, and averaging their absolute values over all 50 replicates. Eigenvectors were ordered and assigned to specific modules depending on the distribution of the trait loadings among them. By trait loadings we mean the elements of the eigenvector, where each is a coordinate on the original trait axes. Co-linearity between each module and its corresponding eigenvector was calculated as:

$$Co - linearity = \frac{\mathbf{Eigenvector} \cdot \mathbf{Module}}{|\mathbf{Eigenvector}||\mathbf{Module}|}, \tag{1}$$

where $\mathbf{Eigenvector} \cdot \mathbf{Module}$ is the dot product of the two vectors, and $|\mathbf{Eigenvector}|$ and $|\mathbf{Module}|$ are their respective norms. Since eigen decomposition arbitrarily assigns positive or negative trait loadings (while creating orthogonal vectors), the absolute values of the trait loadings were used when eigenvectors were being ordered.

Evolutionary Metrics

We used two previously described evolutionary metrics to determine whether they capture the modular structure of the GP map from the **G**-matrix. The first, the effective number of dimensions (n_D) of Kirkpatrick [47], was used to measure the effect of modularity and mutational correlation on the dimensionality of the genetic variance. n_D provides a weighted modularity measure representing the number of independent trait modules with equal variance calculated from the distribution of eigenvalues of the **G**-matrix:

$$n_D = \Sigma_i \frac{\lambda_i}{\lambda_1}, \tag{2}$$

where λ_i is the ith eigenvalue and λ_1 is the largest eigenvalue. The other metric, the average autonomy ($\bar{a}$), was used to evaluate the effect of modularity and mutational correlation on the degree of modular autonomy. The

autonomy of a **G**-matrix measures the lack of correlation between traits [36]. A complete lack of correlation between traits would mean that each trait is essentially its own module (autonomy = 1), whereas complete correlation between traits would mean that all traits are essentially one module (autonomy = 0). The average autonomy, $\bar{a}$, is a general measure of the degree of autonomy over all directions in phenotypic space (since a trait's autonomy is dependent on the direction of selection). We calculated $\bar{a}$ from Hansen & Houle (2009):

$$\bar{a} \approx \frac{H[\lambda]}{E[\lambda]}\left(1 + 2\frac{I[\lambda] + I[1/\lambda] - 1 + H[\lambda]/E[\lambda] + 2I[\lambda]I[1/\lambda]/(k+2)}{k+2}\right), \tag{3}$$

where $H[\lambda]$ is the harmonic mean of eigenvalues ($\frac{1}{E[\frac{1}{\lambda}]}$), $E[\lambda]$ is the arithmetic mean of eigenvalues, $I[\lambda]$ is the mean-standardized variance of eigenvalues $\frac{var[\lambda]}{E[\lambda]^2}$ and k is the number of eigenvalues [36].

Effects of variable pleiotropy on the response to directional selection

While the previous metrics provide an overall assessment of the non-uniformity of the distribution of genetic variance in phenotypic space, and thus of the potential for genetic constraints, they may not fully capture the effect of those constraints on the response to selection in a particular phenotypic direction. To test the capacity of the metrics employed to describe the evolvability (the ability of traits to respond to selection) of a population with a given genetic architecture, we measured the response to directional selection of traits with different GP map modularities. We modeled two adaptive scenarios, one where the position of the phenotypic optimum of the first module is shifted by one phenotypic unit with an equal shift on all traits within the module (i.e., the shift of the optimum value of trait i in a module of size n traits is: $\Delta\theta_i = 1/\sqrt{n}$), and a second where only the first trait of the first module has its optimum shifted by one phenotypic unit. These were applied to the final populations of the previous stabilizing selection simulations (the 10,000th generation). In both regimes, all other traits were subject to stabilizing selection on the same optimum value of 5. We followed the phenotypic trajectory of the populations for 2000 generations by recording the population mean

trait values, $\bar{\mathbf{z}}$, every 10 generations. To evaluate the adaptive capacity of each population, we recorded the number of generations required to surpass the same minimum average fitness threshold set to $\overline{W}$=0.947 (corresponding to population phenotypic distance to optima = 0.726). We averaged all statistics over the 50 replicates performed for each combination of GP map modularity and mutational correlation.

The ability of the metrics to predict evolutionary rate of response to selection was gauged by plotting the results of number of dimensions (n_D), autonomy ($a(\boldsymbol{\beta})$), and evolvability ($e(\boldsymbol{\beta})$) against the number of generations to the average fitness threshold. Autonomy and evolvability along a selection gradient, $a(\boldsymbol{\beta})$ and $e(\boldsymbol{\beta})$ respectively, were used instead of $\bar{a}$ because they represent the autonomy and evolvability with selection in one particular direction (determined by the initial distance and direction to the trait optimum), and were calculated as follows:

$$a(\boldsymbol{\beta}) = \frac{c(\boldsymbol{\beta})}{e(\boldsymbol{\beta})}, \tag{4}$$

$$c(\boldsymbol{\beta}) = (\boldsymbol{\beta}^T \mathbf{G}^{-1} \boldsymbol{\beta})^{-1}, \tag{5}$$

$$e(\boldsymbol{\beta}) = \frac{\boldsymbol{\beta}^T \mathbf{G} \boldsymbol{\beta}}{|\boldsymbol{\beta}|^2}, \tag{6}$$

$$\boldsymbol{\beta} = \frac{-(\bar{\mathbf{z}} - \boldsymbol{\theta})}{\boldsymbol{\omega}^2 + \mathbf{G}} \tag{7}$$

where $\boldsymbol{\beta}$ is the vector of the selection gradient, $\mathbf{G}$ is the $\mathbf{G}$-matrix, $\bar{\mathbf{z}}$ is the vector of population mean trait values, $\boldsymbol{\theta}$ is the vector of optimum trait values, $\boldsymbol{\omega}^2$ is the selection strength matrix, and T is the transpose operator [36].

Results

Effects of pleiotropic modularity from mutational correlation on G-matrix decomposition structure

With zero mutational correlation ($r_\mu = 0$), average eigenvalues show little differences between eigenvectors and are similar among different GP maps,

indicating that genetic variation is distributed almost evenly in all 12 possible dimensions of trait space (Figure 2A). With a non-zero mutational correlation within modules, the highest ranking eigenvalues become noticeably larger than the others indicating that most of the genetic variation lies along fewer dimensions equal to the number of modules in the GP map (Figure 2C and D) and follows the pattern expected when mutational correlation is the sole driver of genetic correlation (Figure S1). The corresponding eigenvectors co-align with the module vectors (Figure 3A). Examination of the trait loadings on the corresponding eigenvectors allows the identification of the genetic modules underlying trait co-variation where the trait loadings cluster according to their module identity in the GP map (Table S1). Module distinction in the distribution of the eigenvalues and orientation of their eigenvectors becomes much weaker when the number of modules increases because the amount of genetic variation captured by each module eigenvector decreases with the number of traits in a module.

Interestingly, modular correlational selection may induce similar modular partitioning of genetic co-variance in the absence of mutational correlation when the GP map is modular (Figure 3B). In absence of modules in the GP map (universal pleiotropy), phenotypic modules in the decomposition of the **G**-matrix appear much weaker (Figure 3C). Modularity in phenotypic variance is more difficult to detect with lower modularity since strong correlational selection reduces the total genetic variance to a greater extent (Figure S2). As in the regime with mutational correlation, the correspondence between trait loadings and trait modules tends to diminish with decreasing strength of correlation (not shown).

Evolutionary metrics

The two evolutionary metrics, effective dimensionality (n_D) and average autonomy ($\bar{a}$), capture the discontinuity of the eigenvalue distribution when mutational correlation is non-zero (Figure 4). Lowest n_D and $\bar{a}$ values are reached for highest mutational correlations and lower modularity (with the exception of modularity 1 in $\bar{a}$), when most traits are genetically correlated with each other. GP maps with less genetic constraints among traits (i.e., smaller r_μ) have highest n_D and $\bar{a}$, to the point where the different GP maps are indistinguishable when mutational correlation is zero (Figure 4). Overall, n_D better captures the variation in modularity of the different GP maps than $\bar{a}$.

Response to directional selection

Regardless of the degree of mutational correlation, when directional selection is imposed on all the traits in one module the average trait values for each trait in that module move closer to the new optimum each generation without much directional deviation (Figure 5A). Populations with higher modularity in their GP map (fewer traits in the module under selection) require fewer generations to reach the same fitness value when mutational correlation is absent but more generations when mutational correlation is present (Figure 5C). Also, when comparing the same GP maps when mutational correlation is present, greater r_μ decreases the number of generations required to reach the same fitness value (Figure 5C). On the other hand, when directional selection is imposed on only one trait in a module, mutational correlation between traits in the same module causes directional deviation of the average trait value of the selected trait (Figure 5B). In this case, populations with higher r_μ require more generations to reach the same fitness value, especially when modularity is low (more traits correlated with the trait under selection) (Figure 5D). Additionally comparing selection regimes, when mutational correlation is absent the resulting values are the same (apart from relatively small stochastically-induced error) regardless of the direction of selection (Figure 5C and D). In contrast, when mutational correlation is present the direction of selection determines whether the average number of generations increases or decreases with increased modularity (Figure 5C and D).

When traits are genetically correlated ($r_\mu > 0$), n_D is positively correlated with generation times to the fitness threshold when selection is on an entire module and negatively correlated when selection is acting on a single trait (Figure 6A and D, respectively). Autonomy along the selection gradient, $a(\boldsymbol{\beta})$, for different modularities is negatively correlated to generation times only when mutational correlation is present and selection is on a *single trait* (Figure 6E). On the other hand evolvability, $e(\boldsymbol{\beta})$, for different modularities is negatively correlated to generation times only when mutational correlation is present and selection is on an *entire module* (Figure 6C). When there is no mutational correlation, and thus little between-trait genetic correlation, the metrics poorly capture the effect of the variation in pleiotropic degree of the mutations on the evolutionary responses of the populations (Figure 6).

Discussion

The predictive utility of the eigen decomposition of a **G**-matrix is dependent on whether there is a meaningful relationship between the eigenvectors and the genetic architecture underlying the **G**-matrix. Here, modular pleiotropy stemming from mutational correlation is evident in the eigenvalue and eigenvector structure, bolstering previous evolutionary quantitative genetic theory about the stabilizing force of mutational correlation on a **G**-matrix and the conditions for the utility of diagonalization for detecting trait groupings [41, 10, 4]. In contrast, a mutational correlation of zero leads to a poor match between a **G**-matrix's eigenvectors and the pleiotropic modules of the traits' GP map because uncorrelated pleiotropic effects do not translate into trait genetic correlations. Indeed, when mutational correlation is zero, no phenotypic correlation should be expected in the first place, unless stemming from random processes [68, 27], gene flow [31], or correlational selection [41, 42, this study]. However, if mutational correlation is strong within modules, stability of the relationship between eigenvectors and genetic modules is assured in most cases, and the eigen decomposition of the **G**-matrix should reflect that of the **M**-matrix.

We further show that correlational selection induces stronger genetic correlation among traits when pleiotropy is modular within the GP map than when it is not; the eigenvectors map to genetic modules when selection is similarly modular. In contrast, universal pleiotropy in the GP map (i.e. absence of pleiotropic modules) hinders the capacity of the eigen decomposition of the **G**-matrix to map modules of elevated trait genetic covariance. In that case, selection was not able to maintain strong within-module correlations in the face of non-correlated mutational effects. Previous models have shown that correlational selection can favor between-trait genetic correlation by selecting on standing genetic co-variation, as we have done [see 41], or by selecting on loci affecting the correlation coefficients within the **M**-matrix [42, 43], or on the pleiotropic degree of the underlying loci, making them more or less pleiotropic [56]. Our results suggest that selection on standing genetic co-variation of universally pleiotropic mutations is the least efficient way of evolving trait phenotypic integration (i.e. elevated correlation within modules). However, if genetic variation for the pleiotropic degree or the mutational correlation of quantitative loci exists in a population, a modular GP map would evolve under correlational selection. Which of the two aspects of pleiotropy evolves faster is not known and may depend on the details of the

genetic systems and the trade-offs associated with gene pleiotropy [e.g. 29]. Recent models and data suggest that genetic variation for trait co-variation may partly depend on epistatic interactions between pleiotropic mutations [67, 66, 43, 65, 69]. In any case, when patterns of trait correlation evolve and are maintained by selection, we should expect stability of both the **M** and **G**-matrix over evolutionary times, and thus of the relationship between phenotypic and genetic modules [e.g., see 56, for stability of trait correlations created by directional selection].

The evolutionary metrics employed also show that the pleiotropic modularity encoded in the GP maps is evident when mutational correlation is present: the distribution of averaged eigenvalues and the trait loadings of their respective eigenvectors, the average number of effective dimensions (n_D), and the average autonomy ($\bar{a}$). The two latter metrics show that they can differentiate high from low modularity of the GP map and can measure the constraints caused by higher mutational correlation but effective dimensionality (n_D) better captures the relative effects of modularity and mutation correlation. In contrast, both metrics are unable to do so in absence of mutational correlation. This is because the within-module correlations do not differ from between-module correlations, and the resulting eigenvalues are almost evenly distributed despite the complete absence of pleiotropic effects across modules. When this is the case (as a result of no mutational correlation), concluding that modularity does not affect the ability of traits to respond to directional selection would, however, be wrong. Indeed, we show that when selecting for a new optimum, larger modules are more constrained than smaller modules, as seen in the increased time they needed to reach higher fitness. This is true whether selection is acting on a whole module or on a single trait within a module and would be true regardless of the direction of selection. The difference in pleiotropic degree among modularities is the reason for this difference here: loci are less pleiotropic in small than large modules and large modules are thus more constrained because lack of directionality in mutations provides smaller net positive effects of beneficial mutations, an effect related to the "cost of complexity" paid by organisms having more traits under selection [e.g. 64, 88]. When pleiotropic mutations are uncorrelated in their effects, metrics based on eigenvalue distributions cannot capture the difference in module size because it does not result in marked differences among eigenvalues. Thus, there are limits to how much can be deduced from the eigen decomposition of the **M**- or **G**-matrix about the structure of the GP map and the evolutionary properties of a set of

quantitative traits.

Our directional selection simulations highlight a caveat when interpreting evolutionary metrics in terms of evolutionary constraints. Clearly, we should always keep in mind that genetic correlations act as constraints only as long as selection is not acting along the eigenvectors of the **G**-matrix. This is well illustrated in our case when selection was acting on a single module, thus aligning the direction of selection with the module's eigenvector. Here, populations with large mutational correlations evolved faster, especially when modularity was low. The explanation is that mutational correlation within larger modules leads to greater genetic variation in the direction of selection, which is evident in a population's evolvability, $e(\boldsymbol{\beta})$. If, on the other hand, the focal trait is the only trait under selection in a module (with all other traits under stabilizing selection) then autonomy along a selection gradient, $a(\boldsymbol{\beta})$, correctly predicts that larger modules evolve slower because the focal trait is genetically linked to more traits. Interestingly, n_D, the effective phenotypic dimensionality of the **G**-matrix, is negatively correlated with $e(\boldsymbol{\beta})$ when selection is on a whole module, reflecting on the case of reduced evolutionary constraints (faster rate of adaptation) in Fisher-Orr model with lower effective dimensionality [see 53]. In contrast, n_D correlates positively with $a(\boldsymbol{\beta})$ when selection is on a single trait, indicating that reduced dimensionality in that case is constraining adaptation. Therefore, n_D, $a(\boldsymbol{\beta})$, and $e(\boldsymbol{\beta})$ are limited in what they can actually say about a trait's ability to respond to new selection regimes because different selection regimes can show constrained or facilitated responses depending on whether the regime selects for correlated mutations (correlated phenotypic changes) or not along a major axis of genetic variation [34, 19, 18].

In sum, our results indicate that we can gain a better understanding of the evolvability of a set of traits, or of an organism, when using evolutionary metrics that capture the two main aspects of genetic constraints among traits; the amount of genetic variation along the direction of selection, captured by $e(\boldsymbol{\beta})$, and the degree of genetic independence of the trait(s) under selection, captured by $a(\boldsymbol{\beta})$. Yet, the metrics used all failed to capture a third important aspect of pleiotropic constraints influencing evolutionary rates; the variation in the pleiotropic degree of the mutations affecting the traits. This failure is most evident when pleiotropic mutational effects are uncorrelated, in which case all metrics have roughly the same value irrespective of the modularity of the GP maps. Our results show that the direction of selection has no effect on rate of adaptation when there is no mutational correlation

(for a particular modularity) but that the degree of pleiotropy has an effect regardless of whether mutational correlation is present or not. Therefore, it is important to keep in mind that similar values of evolutionary metrics across different organisms is not a guarantee that they would evolve at similar rates. Understanding the extent of pleiotropy together with the extent of mutational correlation should thus remain an important goal of empirical studies that seek to unravel the evolutionary properties of natural systems.

Empirical evidence for mutational correlation and modular pleiotropy

The pleiotropic mutational effects in our model abstract out the types of molecular level changes that may lead to genetic correlations observed in **G**-matrices. Correlated mutational effects may arise from mutations that cause correlated effects in more than one of a gene's molecular functions or from mutations causing correlated effects in a gene product's multiple processes but empirical evidence is needed to discover the source of mutational correlation [39, 83]. Even if the specific molecular mechanism that is the cause of correlation is not known it is still possible to estimate the genomic **M**-matrix which describes the combined pattern of (co)variation arising from mutations in all loci that affect the traits of interest. Mutation accumulation experiments in *D. melanogaster* [40] or *C. elegans* [24] provide examples of such genomic **M**-matrix estimates and show the existence of strong mutational correlation among morphological and life-history traits. Additionally, mutational correlations in *C. elegans* seem to correspond to phenotypic correlations among traits after removing environmental correlations and suggest that pleiotropy is somewhat restricted within traits of related function [24]. It is also possible to discover evidence of modular pleiotropy from genome-wide studies using gene knock-out/-down experiments as was performed in yeast [22, 32, 63], *C. elegans* [76], and the house mouse [14], which have shown that whole-gene pleiotropy is variable (does not affect all traits) and often modular [86, 83]. QTL studies further show variable pleiotropy in *D. melanogaster* [60], threespine stickleback [2], the house mouse [16, 45, 61], and *A. thaliana* [44], among others [70]. One empirical study manages to link mutational correlation with modular variation of pleiotropy by measuring both the genomic **M**-matrices and the pleiotropic degree of main and epistatic effects of mutations affecting the replicative capacity (fitness) of HIV-1 in different drug

environments [69]. In doing so, they discovered that epistasis can affect the pleiotropic degree of single mutations producing modular GP maps and that epistatic-pleiotropic effect modules matched modules of fitness co-variation among drugs. These results suggest that epistasis may be fundamental in shaping the GP map itself, which may allow organisms to enhance their evolvability in the face of selection [66].

Caveats

Some of our results are affected by assumptions we made in our model. In particular, we chose to keep the traits' mutational variances (V_m) constant irrespective of module size (i.e. pleiotropic degree) by proportionally adjusting the per-locus mutational variance. This allowed us to compare the response of traits under directional selection with equal genetic variance at mutation-selection equilibrium, but it is certainly not the case that loci in smaller modules have larger effect sizes in real populations [indeed, it may be the opposite, see 82, 86, 70]. Had we kept the per-locus mutational effect variance the same in all sets of modular GP maps, smaller modules (fewer loci affecting fewer traits) would have had lower total genetic variance and, thus, lower rates of adaptation. But smaller effect sizes also mean smaller deleterious side-effects of mutations, which compensate for the effect of reduced variance on rates of adaptation, thus making our results robust to changes in mutational effect sizes (Figure S3). We also chose to model modularity in a simplistic way with the same number of loci affecting the same number of traits overall just varying the pleiotropic degree as the number of modules changed. We could have kept the pleiotropic degree constant with increasing degrees of clustering or used simple allelic vectors with different orientations as in Mezey and Houle [59], but we expect our conclusions to be robust to changes in a GP map structure. Modular correlated pleiotropic effects should lead to modular **G**-matrices, no matter the precise details of the GP map as long as the net pleiotropic effects are correlated across loci.

Although the loci in our model are fully pleiotropic (within their modules) it is likely that most traits in real populations also include loci that are not pleiotropic or are pleiotropic including traits in other modules (e.g. common integrating factors). The more loci that are not fully pleiotropic within a module the worse the correlation between eigenvectors based on genetic correlations and pleiotropic modules are expected to be [28]. But a previous study has shown that even having 25% non-pleiotropic loci in each trait in

the GP map only reduces the correlation between traits down to 0.65 from perfect correlation [8], and when our simulations were run with 20% of loci having full pleiotropy to all traits the modules were still observable in the eigen structure (Figure S4).

The ability to distinguish modules from the eigen decomposition of a population's **G**-matrix diminishes as mutational correlation (or correlational selection) between traits within modules decreases, and would also be diminished by mutational correlations (or correlational selection) between traits in different modules. Drift in small populations is therefore expected to alter our ability to associate eigenvectors with pleiotropic modules because it creates transient trait genetic covariation outside such modules, but a ten-fold decrease in population size does not have an effect on the ability of **G**-matrix decomposition to predict the pleiotropic modularity of the GP map when mutational correlation is present (see Figure S5 and Table S1). Previous findings showed that larger population size lead to greater predictability of the size and shape of a **G**-matrix [41] that allows more precise **G**-matrix measurement [but see 71, for situations where population size fluctuates].

Lastly, we recall that non-equal eigenvalues may stem from non-equal genetic variance among traits, even in the absence of genetic correlations. In our case, drift caused variation among eigenvalues when $r_\mu = 0$ and was also evident when modules of same size differed in their total variance such that the "module" eigenvalues were not all equal (see Figure 2). This variation was however small compared to the variation between "module" and "non-module" eigenvalues because the traits were all on the same scale by design. Trait values should thus be variance-standardized prior to analysis [36] to avoid conflating the effects of variation in trait variances with the effects of trait genetic correlations.

Conclusion

Our study suggests that aspects of the molecular structure of the GP map of quantitative traits can be deduced from the genetic co-variance structure of those traits when such aspects affect the covariation of mutational effects captured by the **M**- and **G**-matrices. In doing so, metrics based on the distribution of eigenvalues or on the geometrical shape of the **G**-matrix may provide an accurate description of the evolutionary properties of a population. For instance, we have shown that $e(\boldsymbol{\beta})$ and $a(\boldsymbol{\beta})$ captured two aspects

of genetic constraints among traits: the amount of genetic variation along the direction of selection and the degree of genetic independence of the trait(s) under selection, respectively. Yet, because variation in the pleiotropic degree of loci in the GP map does not directly affect the shape of a **G**-matrix in the absence of mutational correlation (or correlational selection), evolutionary constraints caused solely by a higher "cost of complexity" of more highly pleiotropic mutations cannot be fully captured by evolutionary metrics based on the shape of a **G**-matrix. Ultimately, the rate of adaptation of a population depends on the distribution of the fitness effects of the mutations affecting the traits under selection, and pleiotropy affects that distribution, reducing the rate of adaptation when mutations affect more of the traits under selection [26, 64, 88, 53, 51]. Therefore, methods that seek to capture the effect of organismal "complexity" on the distribution of fitness effects of mutations may provide a better understanding of evolutionary constraints, although, this is applicable to only a few model organisms.

Acknowledgments: This manuscript benefited from the comments and constructive criticism provided by Daniel Berner, Luis-Miguel Chevin, and two anonymous referees. JC and FG were supported by the Swiss National Science Foundation, grant PP00P3_144846/1 to FG.

References

References

[1] Agrawal, A. F. and Stinchcombe, J. R. (2009). How much do genetic covariances alter the rate of adaptation? *Proc. R. Soc. Lond. (Biol)*, 276(1659):1183–1191.

[2] Albert, A. Y. K., Sawaya, S., Vines, T. H., Knecht, A. K., Miller, C. T., Summers, B. R., Balabhadra, S., Kingsley, D. M., and Schluter, D. (2008). The genetics of adaptive shape shift in stickleback: pleiotropy and effect size. *Evolution*, 62(1):76–85.

[3] Arnold, S. J. (1992). Constraints on phenotypic evolution. *Am. Nat.*, pages S85–S107.

[4] Arnold, S. J., Bürger, R., Hohenlohe, P. A., Ajie, B. A., and Jones, A. G. (2008). Understanding the evolution and stability of the g-matrix. *Evolution*, 62:24512461.

[5] Baatz, M. and Wagner, G. P. (1997). Adaptive inertia caused by hidden pleiotropic effects. *Theor. Popul. Biol.*, 51(1):49–66.

[6] Bégin, M. and Roff, D. A. (2004). From micro- to macroevolution through quantitative genetic variation: Positive evidence from field crickets. *Evolution*, 58(10):2287–2304.

[7] Berner, D. (2011). Size correction in biology: how reliable are approaches based on (common) principal component analysis? *Oecologia*, 166(4):961–971.

[8] Berner, D. (2012). How much can the orientation of g's eigenvectors tell us about genetic constraints? *Ecol. Evol.*, 2:1834–1842.

[9] Berner, D., Stutz, W. E., and Bolnick, D. I. (2010). Foraging trait (co) variances in stickleback evolve deterministically and do not predict trajectories of adaptive diversification. *Evolution*, 64(8):2265–2277.

[10] Blows, M. (2007). A tale of two matrices: multivariate approaches in evolutionary biology. *J. Evol. Biol.*, 20(1):1–8.

[11] Blows, M. W. and Higgie, M. (2003). Genetic constraints on the evolution of mate recognition under natural selection. *Am. Nat.*, 161(2):240–253.

[12] Blows, M. W. and Hoffmann, A. A. (2005). A reassessment of genetic limits to evolutionary change. *Ecology*, 86(6):1371–1384.

[13] Brodie, E. and McGlothlin, J. (2007). A cautionary tale of two matrices: the duality of multivariate abstraction. *J. Evol. Biol.*, 20(1):9–14.

[14] Bult, C. J., Eppig, J. T., Kadin, J. A., Richardson, J. E., Blake, J. A., Group, M. G. D., et al. (2008). The mouse genome database (mgd): mouse biology and model systems. *Nucleic acids research*, 36(suppl 1):D724–D728.

[15] Cheverud, J. M. (1984). Quantitative genetics and developmental constraints on evolution by selection. *J. Theor. Biol.*, 110(2):155–171.

[16] Cheverud, J. M., Routman, E. J., and Irschick, D. J. (1997). Pleiotropic effects of individual gene loci on mandibular morphology. *Evolution*, pages 2006–2016.

[17] Chevin, L.-M., Martin, G., and Lenormand, T. (2010). Fisher's model and the genomics of adaptation: restricted pleiotropy, heterogenous mutation, and parallel evolution. *Evolution*, 64(11):3213–3231.

[18] Conner, J. K. (2012). Quantitative genetic approaches to evolutionary constraint: how useful? *Evolution*, 66(11):3313–3320.

[19] Conner, J. K. and Hartl, D. L. (2004). *A primer of ecological genetics*. Sinauer Associates, Sunderland, MA.

[20] Crow, J. F. and Kimura, M. (1964). The theory of genetic loads. *Proc. XI Int. Congr. Genetics*, 2:495–505.

[21] Draghi, J. A. and Whitlock, M. C. (2012). Phenotypic plasticity facilitates mutational variance, genetic variance, and evolvability along the major axis of environmental variation. *Evolution*, 66(9):2891–2902.

[22] Dudley, A. M., Janse, D. M., Tanay, A., Shamir, R., and Church, G. M. (2005). A global view of pleiotropy and phenotypically derived gene function in yeast. *Molecular systems biology*, 1(1).

[23] Elena, S. F. and Sanjuán, R. (2003). Climb every mountain? *Science*, 302(5653):2074–2075.

[24] Estes, S., Ajie, B. C., Lynch, M., and Phillips, P. C. (2005). Spontaneous mutational correlations for life-history, morphological and behavioral characters in caenorhabditis elegans. *Genetics*, 170(2):645–653.

[25] Falconer, D. S. and Mackay, T. F. (1996). *Introduction to quantitative genetics*. Longman, London, fourth edition.

[26] Fisher, R. A. (1930). *The genetical theory of natural selection: a complete variorum edition*. Oxford University Press.

[27] Griswold, C. K., Logsdon, B., and Gomulkiewicz, R. (2007). Neutral evolution of multiple quantitative characters: a genealogical approach. *Genetics*, 176(1):455–466.

[28] Gromko, M. H. (1995). Unpredictability of correlated response to selection: pleiotropy and sampling interact. *Evolution*, pages 685–693.

[29] Guillaume, F. and Otto, S. P. (2012). Gene functional trade-offs and the evolution of pleiotropy. *Genetics*, 192:1389–1409.

[30] Guillaume, F. and Rougemont, J. (2006). Nemo:an evolutionary and population genetics programming framework. *Bioinformatics*, 22:2556–2557.

[31] Guillaume, F. and Whitlock, M. C. (2007). Effects of migration on the genetic covariance matrix. *Evolution*, 61(10):2398–2409.

[32] Güldener, U., Münsterkötter, M., Kastenmüller, G., Strack, N., van Helden, J., Lemer, C., Richelles, J., Wodak, S. J., García-Martínez, J., Pérez-Ortín, J. E., et al. (2005). Cygd: the comprehensive yeast genome database. *Nucleic acids research*, 33(suppl 1):D364–D368.

[33] Hallgrímsson, B. and Lieberman, D. E. (2008). Mouse models and the evolutionary developmental biology of the skull. *Integ. Compar. Biol.*, 48(3):373–384.

[34] Hansen, T. F. (2003). Is modularity necessary for evolvability?: Remarks on the relationship between pleiotropy and evolvability. *Biosystems*, 69(2):83–94.

[35] Hansen, T. F. (2006). The evolution of genetic architecture. *Ann. Rev. Ecol. Evol. Syst.*, pages 123–157.

[36] Hansen, T. F. and Houle, D. (2008). Measuring and comparing evolvability and constraint in multivariate characters. *J. Evol. Biol.*, 21:1201–1219.

[37] Hansen, T. F. and Houle, D. (2009). Corrigendum. *Journal of Evolutionary Biology*, 22(4):913–915.

[38] Hansen, T. F. and Voje, K. L. (2011). Deviation from the line of least resistance does not exclude genetic constraints: a comment on berner et al.(2010). *Evolution*, 65(6):1821–1822.

[39] Hodgkin, J. (2002). Seven types of pleiotropy. *Int. J. Dev. Biol.*, 42(3):501–505.

[40] Houle, D. and Fierst, J. (2013). Properties of spontaneous mutational variance and covariance for wing size and shape in Drosophila melanogaster. *Evolution*, 67(4):1116–1130.

[41] Jones, A. G., Arnold, S. J., and Bürger, R. (2003). Stability of the g-matrix in a population experiencing pleiotropic mutation, stabilizing selection, and genetic drift. *Evolution*, 57:1747–1760.

[42] Jones, A. G., Arnold, S. J., and Bürger, R. (2007). The mutation matrix and the evolution of evolvability. *Evolution*, 61(4):727–745.

[43] Jones, A. G., Bürger, R., and Arnold, S. J. (2014). Epistasis and natural selection shape the mutational architecture of complex traits. *Nat. Comm.*, 5.

[44] Juenger, T., Perez-Perez, J. M., Bernal, S., and Micol, J. L. (2005). Quantitative trait loci mapping of floral and leaf morphology traits in Arabidopsis thaliana: evidence for modular genetic architecture. *Evol. Dev.*, 7(3):259–271.

[45] Kenney-Hunt, J. P., Wang, B., Norgard, E. A., Fawcett, G., Falk, D., Pletscher, L. S., Jarvis, J. P., Roseman, C., Wolf, J., and Cheverud, J. M. (2008). Pleiotropic patterns of quantitative trait loci for 70 murine skeletal traits. *Genetics*, 178(4):2275–2288.

[46] Kingsolver, J. G., Hoekstra, H. E., Hoekstra, J. M., Berrigan, D., Vignieri, S. N., Hill, C. E., Hoang, A., Gibert, P., and Beerli, P. (2001). The strength of phenotypic selection in natural populations. *Am. Nat.*, 157(3):245–261.

[47] Kirkpatrick, M. (2009). Patterns of quantitative genetic variation in multiple dimensions. *Genetica*, 136:271–284.

[48] Lande, R. (1979). Quantitative genetic analysis of multivariate evolution, applied to brain:body size allometry. *Evolution*, 33:402416.

[49] Lande, R. (1980). The genetic covariance between characters maintained by pleiotropic mutations. *Genetics*, 94(1):203–215.

[50] Lande, R. and Arnold, S. J. (1983). The measurement of selection on correlated characters. *Evolution*, pages 1210–1226.

[51] Lourenço, J., Galtier, N., and Glémin, S. (2011). Complexity, pleiotropy, and the fitness effect of mutations. *Evolution*, 65:1559–1571.

[52] Marroig, G. and Cheverud, J. M. (2005). Size as a line of least evolutionary resistance: Diet and adaptive morphological radiation in new world monkeys. *Evolution*, 59(5):1128–1142.

[53] Martin, G. and Lenormand, T. (2006). A general multivariate extension of fisher's geometrical model and the distribution of mutation fitness effects across species. *Evolution*, 60(5):893–907.

[54] Maynard Smith, J., Burian, R., Kauffman, S., Alberch, P., Campbell, J., Goodwin, B., Lande, R., Raup, D., and Wolpert, L. (1985). Developmental constraints and evolution: a perspective from the mountain lake conference on development and evolution. *Q. Rev. Biol.*, pages 265–287.

[55] McGuigan, K., Chenoweth, S. F., and Blows, M. W. (2005). Phenotypic divergence along lines of genetic variance. *Am. Nat.*, 165(1):32–43.

[56] Melo, D. and Marroig, G. (2015). Directional selection can drive the evolution of modularity in complex traits. *Proc. Natl. Acad. Sci. U.S.A.*, 112:470–475.

[57] Merila, J. and Bjorklund, M. (1999). Population divergence and morphometric integration in the greenfinch (carduelis chloris) - evolution against the trajectory of least resistance? *J. Evol. Biol.*, 12(1):103–112.

[58] Mezey, J. G., Cheverud, J. M., and Wagner, G. P. (2000). Is the genotype-phenotype map modular?: a statistical approach using mouse quantitative trait loci data. *Genetics*, 156(1):305–311.

[59] Mezey, J. G. and Houle, D. (2003). Comparing g matrices: Are common principle components informative? *Genetics*, 165:411425.

[60] Mezey, J. G., Houle, D., and Nuzhdin, S. V. (2005). Naturally segregating quantitative trait loci affecting wing shape of drosophila melanogaster. *Genetics*, 169(4):2101–2113.

[61] Miller, C. T., Glazer, A. M., Summers, B. R., Blackman, B. K., Norman, A. R., Shapiro, M. D., Cole, B. L., Peichel, C. L., Schluter, D., and Kingsley, D. M. (2014). Modular skeletal evolution in sticklebacks is controlled by additive and clustered quantitative trait loci. *Genetics*, 197(1):405–420.

[62] Mitchell-Olds, T. (1996). Pleiotropy causes long-term genetic constraints on life-history evolution in brassica rapa. *Evolution*, pages 1849–1858.

[63] Ohya, Y., Sese, J., Yukawa, M., Sano, F., Nakatani, Y., Saito, T. L., Saka, A., Fukuda, T., Ishihara, S., Oka, S., et al. (2005). High-dimensional and large-scale phenotyping of yeast mutants. *Proceedings of the National Academy of Sciences of the United States of America*, 102(52):19015–19020.

[64] Orr, H. A. (2000). Adaptation and the cost of complexity. *Evolution*, 54(1):13–20.

[65] Pavlicev, M. and Cheverud, J. M. (2015). Constraints evolve: context dependency of gene effects allows evolution of pleiotropy. *Ann. Rev. Ecol. Evol. Syst.*, 46:413–434.

[66] Pavlicev, M., Cheverud, J. M., and Wagner, G. P. (2010). Evolution of adaptive phenotypic variation patterns by direct selection for evolvability. *Proceedings of the Royal Society of London B: Biological Sciences*, page rspb20102113.

[67] Pavlicev, M., Kenney-Hunt, J. P., Norgard, E. A., Roseman, C. C., Wolf, J. B., and Cheverud, J. M. (2008). Genetic variation in pleiotropy: differential epistasis as a source of variation in the allometric relationship between long bone lengths and body weight. *Evolution*, 62(1):199–213.

[68] Phillips, P. C., Whitlock, M. C., and Fowler, K. (2001). Inbreeding changes the shape of the genetic covariance matrix in drosophila melanogaster. *Genetics*, 158(3):1137–1145.

[69] Polster, R., Petropoulos, C. J., Bonhoeffer, S., and Guillaume, F. (2016). Epistasis and pleiotropy affect the modularity of the genotype–phenotype map of cross-resistance in hiv-1. *Molecular Biology and Evolution*, 33(12):3213–3225.

[70] Porto, A., Schmelter, R., VandeBerg, J. L., Marroig, G., and Cheverud, J. M. (2016). Evolution of the genotype-to-phenotype map and the cost of pleiotropy in mammals. *Genetics*, 204(4):1601–1612.

[71] Revell, L. J. (2007). The g matrix under fluctuating correlational mutation and selection. *Evolution*, 61(8):1857–1872.

[72] Roff, D. A. (1996). The evolution of genetic correlations: an analysis of patterns. *Evolution*, pages 1392–1403.

[73] Roseman, C. C., Kenny-Hunt, J. P., and Cheverud, J. M. (2009). Phenotypic integration without modularity: testing hypotheses about the distribution of pleiotropic quantitative trait loci in a continuous space. *Evol. Biol.*, 36(3):282–291.

[74] Schluter, D. (1996). Adaptive radiation along genetic lines of least resistance. *Evolution*, 50:1766–1774.

[75] Simon, M. N., Machado, F. A., and Marroig, G. (2016). High evolutionary constraints limited adaptive responses to past climate changes in toad skulls. *Proc. R. Soc. Lond. (Biol)*, 283(1841):20161783.

[76] Sönnichsen, B., Koski, L., Walsh, A., Marschall, P., Neumann, B., Brehm, M., Alleaume, A.-M., Artelt, J., Bettencourt, P., Cassin, E., et al. (2005). Full-genome rnai profiling of early embryogenesis in caenorhabditis elegans. *Nature*, 434(7032):462–469.

[77] Steppan, S. J., Phillips, P. C., and Houle, D. (2002). Comparative quantitative genetics: evolution of the g matrix. *Trends Ecol. Evol.*, 17(7):320–327.

[78] Turelli, M. (1985). Effects of pleiotropy on predictions concerning mutation-selection balance for polygenic traits. *Genetics*, 111(1):165–195.

[79] Turelli, M. (1988). Phenotypic evolution, constant covariances, and the maintenance of additive variances. *Evolution*, 42(6):1342–1347.

[80] Wagner, G. P. (1989). Multivariate mutation-selection balance with constrained pleiotropic effects. *Genetics*, 122(1):223–234.

[81] Wagner, G. P. and Altenberg, L. (1996). Perspective: complex adaptations and the evolution of evolvability. *Evolution*, page 967976.

[82] Wagner, G. P., Kenney-Hunt, J. P., Pavlicev, M., Peck, J. R., Waxman, D., and Cheverud, J. M. (2008). Pleiotropic scaling of gene effects and the 'cost of complexity'. *Nature*, 452(7186):470–472.

[83] Wagner, G. P. and Zhang, J. (2011). The pleiotropic structure of the genotype–phenotype map: the evolvability of complex organisms. *Nat. Rev. Genet.*, 12(3):204–213.

[84] Walling, C. A., Morrissey, M. B., Foerster, K., Clutton-Brock, T. H., Pemberton, J. M., and Kruuk, L. E. B. (2014). A multivariate analysis of genetic constraints to life history evolution in a wild population of red deer. *Genetics*, 198(4):1735–1749.

[85] Walsh, B. and Blows, M. W. (2009). Abundant genetic variation + strong selection = multivariate genetic constraints: A geometric view of adaptation. *Annu. Rev. Ecol. Evol. Syst.*, 40(1):41–59.

[86] Wang, Z., Liao, B. Y., and Zhang, J. Z. (2010). Genomic patterns of pleiotropy and the evolution of complexity. *Proc. Natl. Acad. Sci. U.S.A.*, 107:18034–18039.

[87] Watson, R. A., Wagner, G. P., Pavlicev, M., Weinreich, D. M., and Mills, R. (2014). The evolution of phenotypic correlations and developmental memory. *Evolution*, 68(4):1124–1138.

[88] Welch, J. J., Waxman, D., and Houle, D. (2003). Modularity and the cost of complexity. *Evolution*, 57(8):1723–1734.

[89] Williams, G. C. (1957). Pleiotropy, natural selection, and the evolution of senescence. *Evolution*, 11(4):398–411.

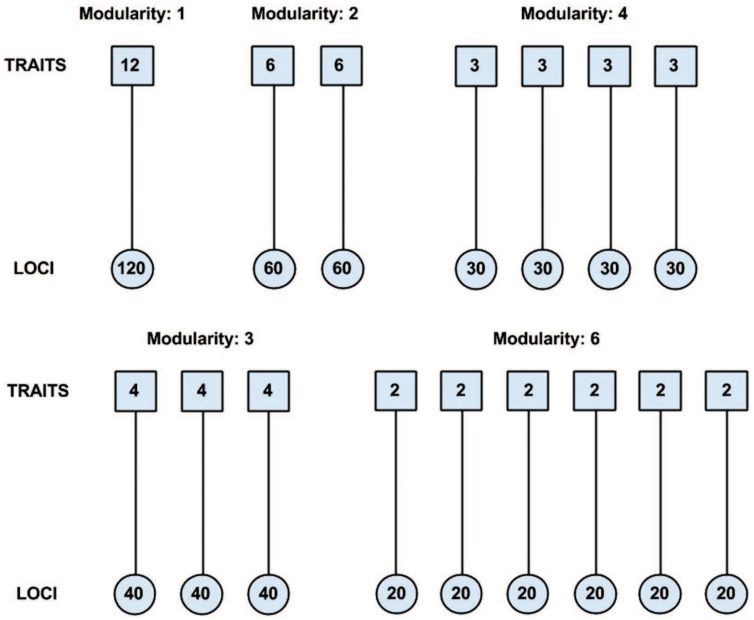

Figure 1: Five different GP map sets showing pleiotropic modules with number of loci (circles) connected to all traits (squares) within each module in each set.

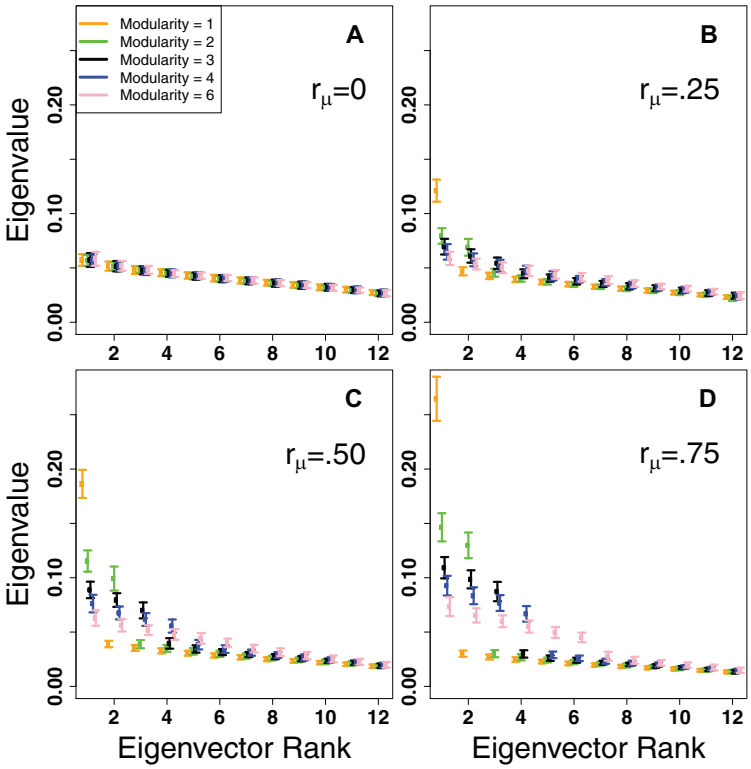

Figure 2: Average eigenvalues of the **G**-matrix with their standard deviations for simulation runs with different degrees of mutational correlation (r_μ) and pleiotropic modularities. Colours represent different pleiotropic modularities (Orange=Modularity 1; Green=Modularity 2; Black=Modularity 3; Blue=Modularity 4; Pink=Modularity 6). Data points are slightly offset for better visualization.

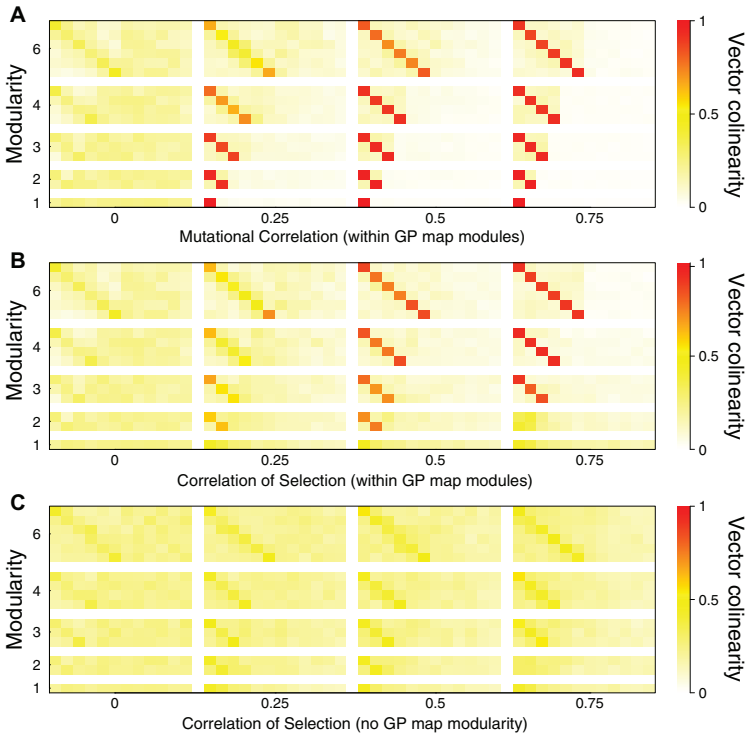

Figure 3: Average cosine of angles between eigenvectors (columns) and modules (rows) for simulation runs with different degrees of mutational correlation (r_μ), correlational selection and pleiotropic modularities (A – No correlational selection, B – No mutational correlation (r_μ=0) but with modular correlational selection within modular GP map, C – No mutational correlation (r_μ=0) or modular GP map but with modular correlational selection). Colours represent cosine of angle between GP map modules and eigenvectors of **G**-matrix: Red – $cos(\theta) = 1$ (Co-linear); White – $cos(\theta) = 0$ (Orthogonal).

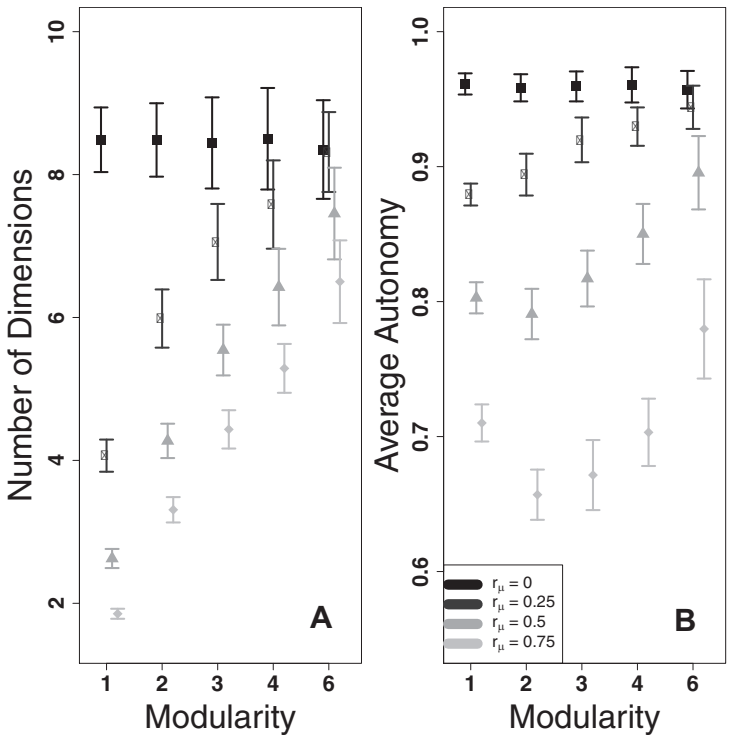

Figure 4: Effective number of dimensions (n_D) and average autonomy ($\bar{a}$) with their standard deviations for simulation runs with different mutational correlations (r_μ) and pleiotropic modularities. Shades of grey represent different degrees of mutational correlation (Darkest grey=0; Dark grey=0.25; Light grey=0.5; Lightest grey=0.75). Data points are slightly offset for better visualization

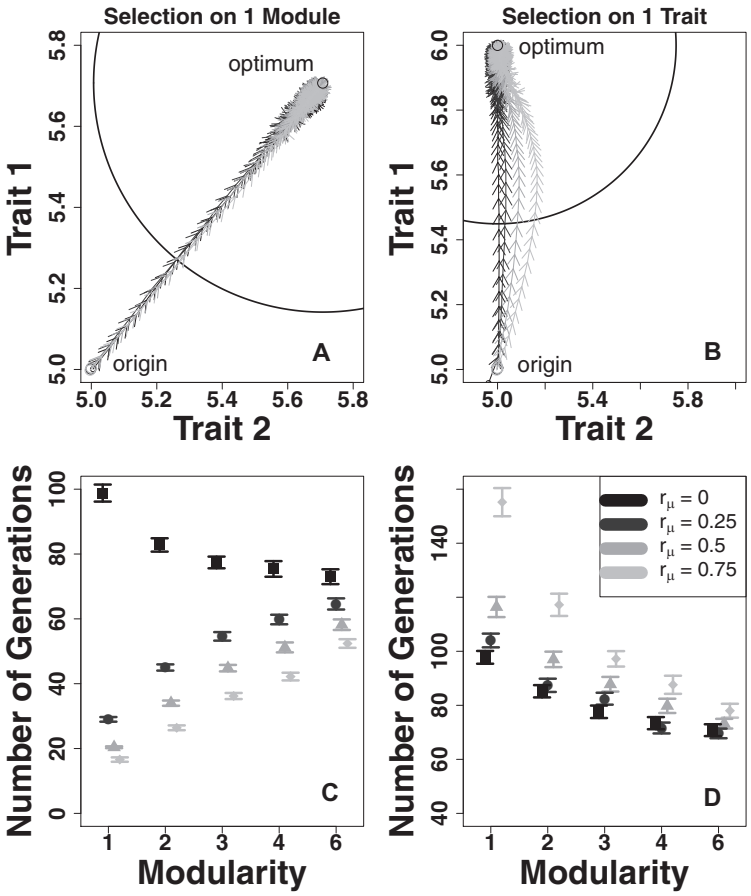

Figure 5: Average trait values of trait 1 and 2 (both in the same module) plotted every 10 generations for 2000 generations (A and B) from simulations with a modularity of 6 and either directional selection on both traits in one module (A and C) or directional selection on trait 1 in one module (B and D). Large circles represent positions at which combined trait values of trait 1 and 2 have a fitness of 0.947 (when all other traits have a value of 5). Average number of generations at which populations surpassed an average fitness of 0.947 (Distances to optima = 0.726) with their standard deviations (C and D). Shades of grey represent different degrees of mutational correlation (Darkest grey=0; Dark grey=0.25; Light grey=0.5; Lightest grey=0.75). Data points are slightly offset for better visualization.

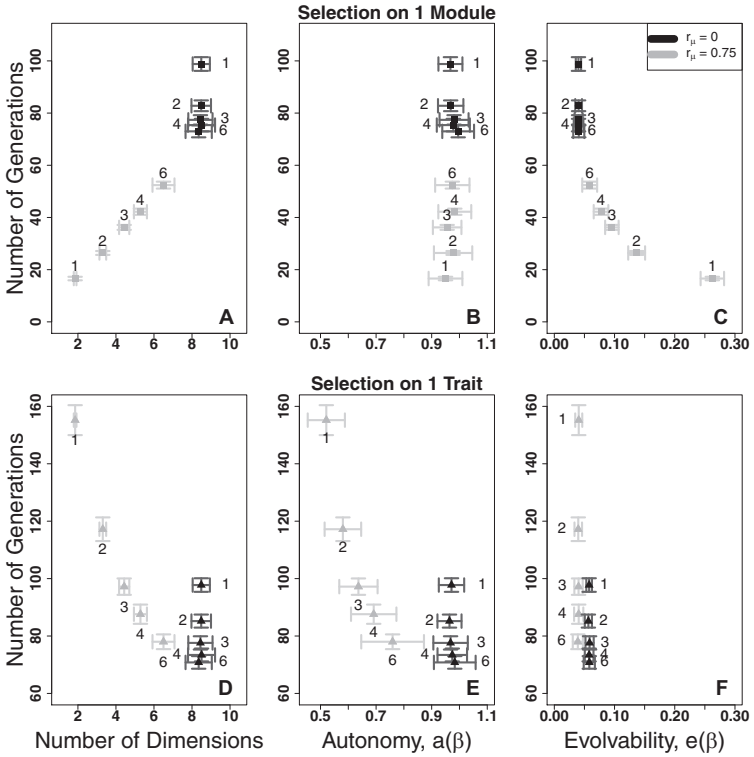

Figure 6: Average effective number of dimensions (n_D), autonomy ($a(\boldsymbol{\beta})$) and evolvability ($e(\boldsymbol{\beta})$) along a selection gradient (determined by the initial distance and direction to the trait optimum), with their standard deviations, plotted against number of generations with selection on one module (A–C) or selection on one trait (D–F), with and without mutational correlation (r_μ), and with different pleiotropic modularities (numbered 1 to 6). Shades of grey represent different degrees of mutational correlation (Dark grey=0; Light grey=0.75). Data points in the case of r_μ=0 (F) are offset by +0.017 on the $e(\boldsymbol{\beta})$ axis for better visualization.